

Article

Degradation of Epoxy–Particles Composites Exposed to UV and Gamma Radiation

Mauricio Torres ^{1,*} , Louise Burdin ² , A. Victoria Rentería-Rodríguez ³ and Edgar A. Franco-Urquiza ³ 

¹ Mechanical Engineering Department, Center for Engineering and Industrial Development, CIDESI, Pie de la Cuesta 702, Queretaro 76125, Mexico

² Faculté de Chimie, CPE Lyon, 69 100 Villeurbanne, France

³ Manufacturing Engineering Department, Center for Engineering and Industrial Development, CIDESI, Pie de la Cuesta 702, Queretaro 76125, Mexico

* Correspondence: mauricio.torres@cidesi.edu.mx; Tel.: +52-442-211-9800 (ext. 5333)

Abstract: In the design and fabrication of any structural system for space application, balance between mass, stiffness and strength is crucial. Structures in space environments are exposed to high radiation levels and thermal shock, due to the sun irradiance and rotation around Earth. Therefore, accurate determination of the thermal and radiation properties is a key issue for the materials used in such applications. This study reports the thermal and mechanical performance of particle composites (epoxy resin and ZnO particles) after gamma and UV radiation. Composites are exposed to gamma and UV radiation at rates of 1 kGy and 10 kGy and characterized after exposure. For the evaluation, DMA, TGA and three-point bending mechanical test are performed to determine thermal properties and possible material degradation after radiation exposure. The incorporation of the filler in the thermal, radiation and mechanical response of the epoxy system improves as a function of its concentration. Then, epoxy resin reinforced with ZnO particles can be a potential candidate as a polymeric matrix for fiber-reinforced composites for nanosatellites.

Keywords: epoxy; ZnO; radiation; mechanical test; loss modulus



Citation: Torres, M.; Burdin, L.; Rentería-Rodríguez, A.V.; Franco-Urquiza, E.A. Degradation of Epoxy–Particles Composites Exposed to UV and Gamma Radiation. *Chemistry* **2023**, *5*, 559–570. <https://doi.org/10.3390/chemistry5010040>

Academic Editor: Edwin Charles Constable

Received: 23 December 2022

Revised: 8 February 2023

Accepted: 2 March 2023

Published: 8 March 2023



Copyright: © 2023 by the authors. Licensee MDPI, Basel, Switzerland. This article is an open access article distributed under the terms and conditions of the Creative Commons Attribution (CC BY) license (<https://creativecommons.org/licenses/by/4.0/>).

1. Introduction

Composite materials are currently replacing metals in the field of aeronautics and aerospace. They have advantages in terms of mass and strength. In addition, it is possible to obtain the desired stiffness with the appropriate type of fiber as well as its orientation within the composite material [1–3].

Polymer composites are formed by two phases: (i) polymer matrix and (ii) fiber reinforcement, the first one is selected in terms of its strength to environmental conditions and the second in terms of its carry loading capacity.

The polymer matrices commonly used are thermoset resins. Those have an excellent thermal and mechanical behavior, as their T_g is usually above 60 °C. Additionally, they have an acceptable good radiation strength (UV rays, gamma rays) when they are exposed to daylight environments. Nonetheless, there are some applications where composites are desired but thermal and irradiation conditions surpass their natural limits [4]. The impact of cumulative radiation damage to materials is commonly measured in terms of the Total Ionizing Dose (TID), expressed in Gray (Gy). UV and gamma irradiation penetrate intensely, causing aging of resins by molecular chain scission and free-radical production. UV and gamma degradation combined with oxygen produces hydroxyl and peroxy radicals as well as water molecules, a process named photo-oxidation. Likewise, irradiation also prompts thermal degradation, which accelerates the reduction of mechanical properties.

As an example, nowadays there are efforts to employ composites as structural materials for CubeSat nanosatellites. CubeSats are 10 × 10 × 10 cm satellites made of aluminum alloys [5,6]. Space agencies are exploring substitution of Al alloys to (i) improve payload

and (ii) assure lifetime in space for the required mission [7]. Thus, the objective is to find a composite material with at least the thermal and loading properties of aluminum but reducing the weight of the satellite [6]. CubeSats in their space mission must deal with vacuum, radiation (UV and gamma) and thermal loading. According to NASA, for low-orbit Earth, below an altitude of 2000 km, radiation estimation is about 2 kGy/year (2×10^5 rads/year) [8–10]. Currently, CubeSat missions are designed to last from 1 to 5 years, then the accumulated radiation dose for these spacecrafts will be at least 10 kGy. It is for this reason that the performance of thermoset resins for the composite candidates, under the cited conditions, is now currently studied [11,12].

Another current application, where high energy causes harsh radiation environments, are the efforts of today's Large Hadron Collider (LHC). Estimations are calculated such that the total cumulated radiation over 10 years of operation can reach 10 kGy. Some studies have reported the damage on thermoset polymers, such as poly(methylmethacrylate) (PMMA), used on optical devices for measuring radiation when it reaches 1.8 MGy [13,14]. Radiation causes compaction and densification of thermoset polymers. On one hand, compaction may modify the geometry of the component; on the other hand, densification can alter the mechanical properties of the device [13]. Even with those drawbacks, optical devices (called LOF—Lab-on-Fiber) exposed to protons at high fluence levels (23 GeV proton beam for 9 days producing a cumulated dose of 1.8 MGy) did not produce a strong degradation of the wavelength spectrum, 1.4 nm of resonance wavelength shift, demonstrating the radiation resistance feature of the device and the material used.

Recent studies have proposed the use of nanoparticles as reinforcements to improve thermal, electrical and harsh resistance. Typically, metal oxides (ZnO, CaO, metakaolin, UIO-66-OH) [15–20] and carbon-based materials (carbon nanotubes, graphene oxide, etc.) [21,22] have shown promising features as thermal reinforcements due to their natural ceramic properties. On one hand, metal oxide particles are good UV absorbers for superficial radiation; nonetheless, after long-term exposures, they suffer from weak targeted scavenging when free radicals are generated. On the other hand, carbon-based materials have good antioxidant performance when hydroxyl and peroxy radicals are formed; however, their irradiation stability depends on their number of defects and porosity [21].

From all these options, ZnO stands out as the most used because of its (i) ease to synthesize, (ii) cost–benefit ratio and (iii) absorption of UVR between 290 and 400 nm (whole range of UVA and UVB) to protect the polymer from full UV degradation. ZnO has additionally a refractive index in visible light of 1.9 resulting in a good light transmissibility. For all these reasons, it has been used as an irradiation inhibitor in cosmetics, sunscreen and clothing. Even adding low doses of ZnO, less than 4 wt%, is enough to block UVA and UVB of exposed materials [18–20].

This study focuses on an epoxy resin to which ZnO particles have been incorporated. This resin was exposed to UV and gamma radiation and then subjected to various analysis techniques (DMA, TGA and bending tests). The goal is to place the resin in an environment that it could face in space in order to be able to characterize its degradation after exposure. The mechanical and thermal properties are therefore studied before and after exposure in order to determine whether the resin has the properties required to be used for the construction of the CubeSat nanosatellite.

2. Materials and Methods

2.1. Synthesis of Zinc Oxide Particles

To produce the zinc oxide particles, the procedure is as follows: The graduated burette contains a solution of sodium hydroxide (2 g) and ethanol (500 mL) which has been homogenized beforehand. Zinc acetate (10.975 g) and then ethanol (500 mL) were added to the three-necked flask and mixed until the temperature reached between 65 and 75 °C. After waiting for 15 min, the NaOH was added drop by drop to maintain the temperature [23,24].

The solution obtained was then dried in an oven and washed 2 or 3 times with distilled water. Then, the solution was placed in an ultrasonic bath to homogenize it before drying it

one last time. Finally, the product obtained was triturated using a mortar to obtain a very fine powder. With this recipe, 2.6895 g of zinc oxide particles was obtained in the form of a white-gray powder.

2.2. Epoxy Resin

Epoxy resin used on this work is EPOLAM 2015 from Sika® (San Luis Potosi, Mexico) and its properties are cited in Table 1.

Table 1. Epoxy resin used in ZnO-epoxy composites.

Property	Value ¹
Density cured (kg/m ³)	1.08
Mixing ratio by weight	100/32
T _g (°C)	88
Curing (h @ °C)	24 @ 25 °C
Viscosity mixed at 25 °C (mPa·s)	550
Pot life (500 g) at 25 °C (min)	140

¹ All values from material's data sheet.

2.3. Preparation of the Resin Containing Zinc Oxide Particles

To produce the particle–resin composite, the procedure is as follows: In a first step, the desired amount of ZnO particles were suspended in ethanol and sonicated for about 5 min to break the agglomerates as much as possible and until a homogeneous dispersion was achieved. Then, the epoxy resin (59 g resin with 11 g of hardener, mix ratio = 6 to 1) was added to the solution that was kept under constant stirring at 50 °C in an ultrasonic bath, until ethanol was completely evaporated, and apparent uniform distribution of the ZnO in the resin was attained. Finally, the composite mixture was placed in silicone molds and left to harden for at least 4 days at room temperature. Before carrying out the various analyses, it was necessary to polish the coupons. Three families of coupons were fabricated with 0.1%, 0.25% and 0.5 wt% of ZnO.

2.4. Exposure to Gamma Radiation

Epoxy-ZnO samples were exposed to gamma irradiation at doses of 10 kGy. The radiation dose is equivalent to 10 times the average CubeSat debris time which is 25 years. The irradiation source was an MDS Nordion Gammacell 220 Excel irradiator with Co60 radiation source. The irradiation medium of the samples was air (Figure 1).

2.5. Thermal Characterization

Thermal characterization was carried out by a 4000 Perkin Elmer TGA with the following parameters: (i) 2 min at 25 °C, (ii) heating from 25 °C to 600 °C at 10 °C/min in Nitrogen and (iii) heating from 600 °C to 750 °C, at 10 °C/min with Oxygen.

Additionally, mechanical-dynamic analysis was set up with a TA Instruments DMA 850 in single cantilever mode at 1 Hz, by heating from 25 °C to 130 °C, at 5°C/min.

2.6. Mechanical Characterization

Three-point bending tests were performed following procedure A of ASTM D7264 standard in order to determine the flexural properties of the epoxy resin and the epoxy–ZnO composites. A universal MTS Insight Electromechanical 100 kN LPS 304 testing machine was employed (Figure 2). The nominal dimensions of the beam coupons were 125 × 12 × 3.5 mm. The support span was fixed on 64 mm (16 times the thickness), with a loading point at the middle length of the coupon. All bending tests were carried out at a displacement rate of 2 mm/min until the coupon failure was reached.

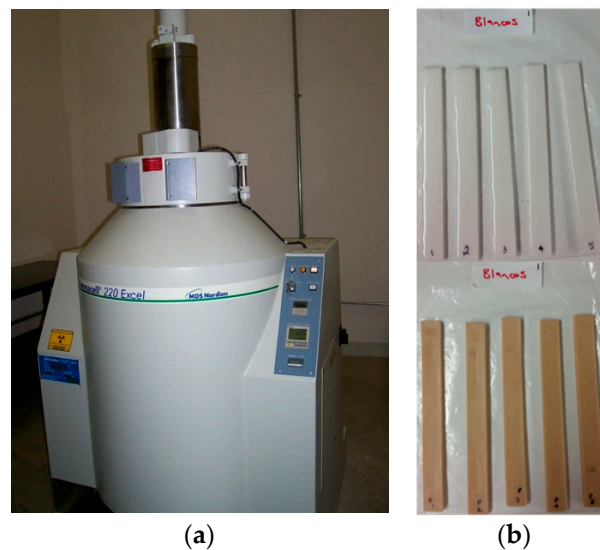


Figure 1. (a) MDS Nordion Gammacell 220 Excel irradiator (courtesy of UNISON, México); (b) ZnO-epoxy composite samples before (white) and after (brown) UV and gamma irradiation.

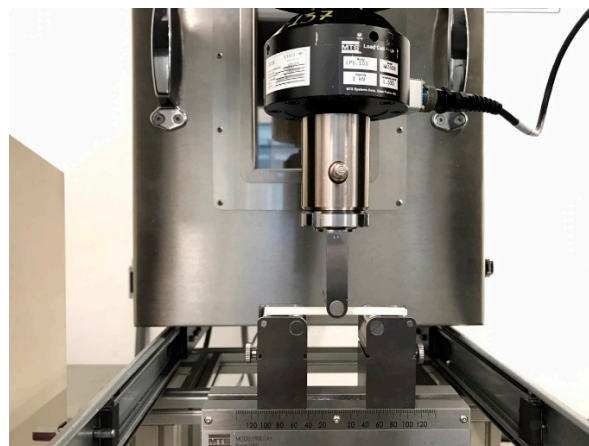


Figure 2. ASTM D7264 mechanical test of ZnO-epoxy composites.

For all characterization techniques, each group of samples was tested five times to ensure the reliability of the data.

3. Results

3.1. Morphology of Zinc Oxide Particles

After synthesizing ZnO particles, SEM micrographs were taken to describe their morphology and size. Figure 3 shows that the ZnO particles are small cubic and irregular chunks, but also spheroids can be observed, with a range of size from 100 nm to 500 nm. A more detailed characterization can be found in [24].

The appearance of all samples after UV and gamma irradiation was dark yellow-brown color. A complete characterization of colorimetry analysis to determine lightness (L^*), chromaticity (C^*) and Hue angle ($^\circ\text{Hue}$) can be found in [15].

3.2. Thermal Performance of Epoxy-ZnO Composite

The thermal properties of the epoxy resin and composites were measured by thermogravimetric analysis (TGA). The effect of the irradiation treatment on thermal stability is shown in Tables 2 and 3.

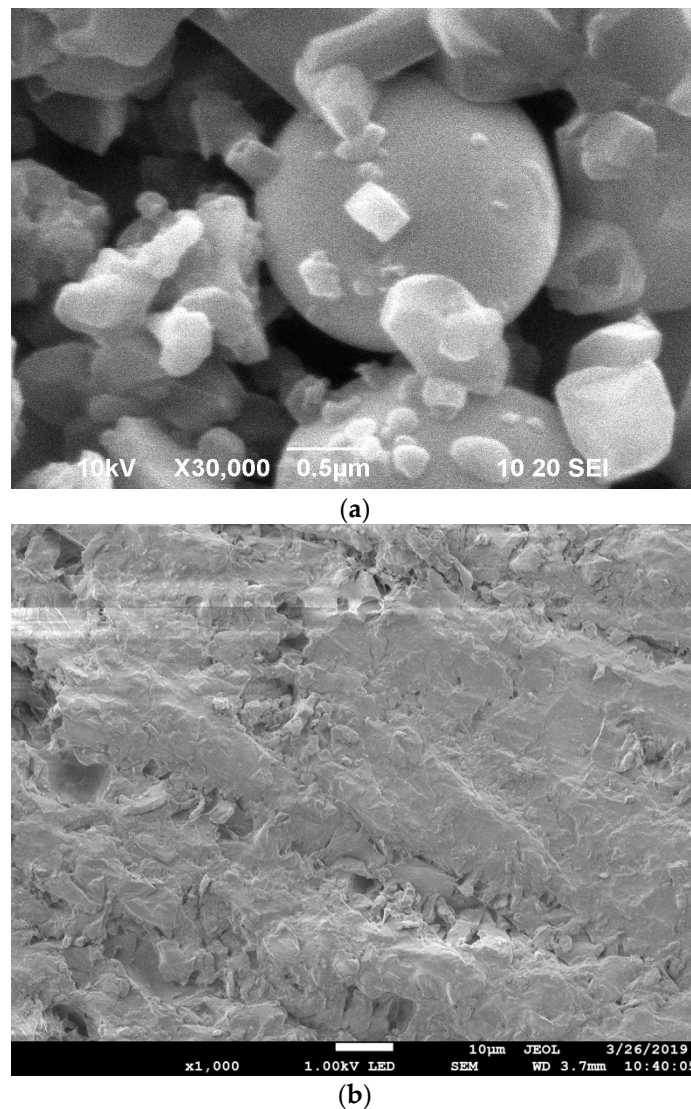


Figure 3. (a) Morphology of ZnO-epoxy particles, (b) integration of ZnO in epoxy resin (0.5 wt%).

Table 2. Temperature pics of the TGA derivative for epoxy-ZnO composites before irradiation.

Composite	1st Pic (°C)	2nd Pic (°C)	3rd Pic (°C)
Neat epoxy	342.65	518.71	692.82
0.1%	343.65	521.81	706.07
0.25%	343.95	520.43	701.25
0.5%	344.81	521.64	698.54

Table 3. Temperature pics of the TGA derivative for epoxy-ZnO composites after irradiation.

Composite	1st Pic (°C)	2nd Pic (°C)	3rd Pic (°C)
Neat epoxy	335.57	514.31	658.53
0.1%	343.98	516.22	699.44
0.25%	337.00	523.69	690.97
0.5%	342.40	516.39	683.71

The initial thermal decomposition temperature (T_{d1} —1st pic), defined as the temperature at which the TGA curve starts to deviate from the baseline point, can be obtained. The irradiation treatment influences the thermal stability of neat epoxy and composites [25].

Tables 2 and 3 show that the T_{d1} (1st pic) of the epoxy-ZnO composites increases at least 1.5 °C from 335.57 °C (neat epoxy), reaching a maximum increment of almost 10 °C (0.1 wt% ZnO). Another temperature (T_{d2} —2nd pic) can be obtained during the decomposition of the composite. For instance, the T_{d2} of the composites is at least 2 °C higher than 514.31 °C (neat epoxy), having a maximum increment of 11 °C (0.25 wt% ZnO). Finally, the last temperature obtained (T_{dmax} —3rd pic) is when the maximum thermal decomposition rate is reached. T_{dmax} for all composites was higher than neat epoxy. The temperature decreased as the ZnO content increased from 706.07 °C up to 698.54 °C.

After samples were irradiated, the T_{d1} of the epoxy-ZnO composites remained higher, at least 1.3 °C from 342.65 °C (neat epoxy), reaching a maximum increment of 2.1 °C (0.5 wt% ZnO). The T_{d2} of the composites shows an average increment of 3 °C compared to 518.71 °C (neat epoxy). The irradiation treatment affects thermal stability. T_{dmax} was notoriously lower than untreated samples. The ZnO particles do not alter the influence of the thermal treatment; hence the T_{dmax} of the composites with 0.1 and 0.5 wt% ZnO particles was significantly lower (11 °C and 15 °C, respectively) than untreated samples.

Figure 4 presents the derived thermogravimetric analysis (DTG) plots corresponding to neat epoxy and composites. In all cases, the presence of a signal at about 100 °C was assigned to the elimination of water molecules.

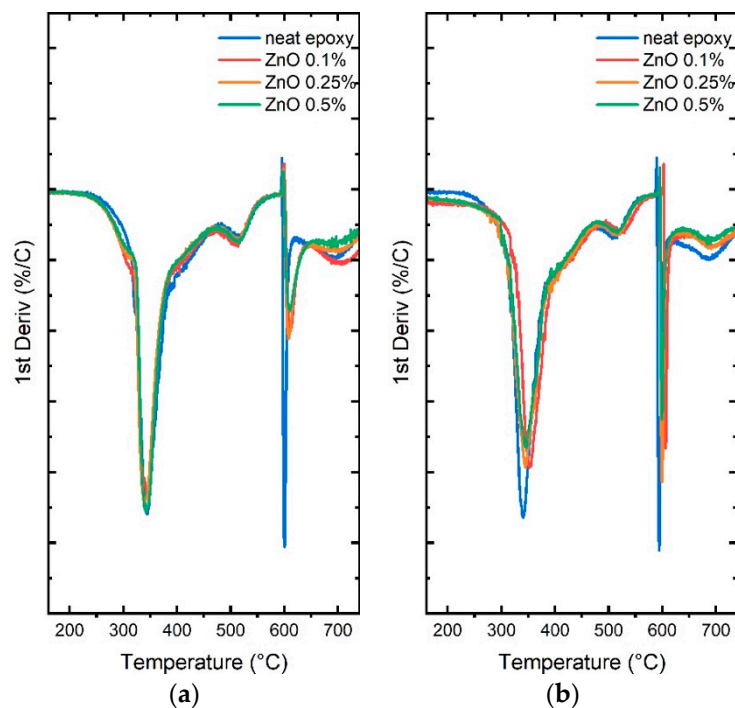


Figure 4. DTG plots corresponding to (a) epoxy-ZnO composites before irradiation, (b) epoxy-ZnO composites after irradiation.

As reported before, the epoxy-ZnO composites show a three-phase degradation influenced by the nanofiller's content [24].

The first peak in the temperature ranges from 300 to 380 °C is related to the primary devolatilization, that is, the release of volatile substances [26]. Some authors described similar ranges with initial degradation due to the loss of mass due to dehydration of the water [27]. Additionally, this phase is associated with uncured resin and loss of volatiles. The addition of ceramic particles delays the first degradation phase, helping with volatiles' dissipation. The second peak in the temperature range from 480 to 560 °C is assigned to secondary devolatilization that mainly involves a release of hydrogen and methane [26], as well as polymer chain scission that takes place progressively along the main chain until the fragments are small enough to volatilize [27]. In this region, organic

compounds' carbonization leads to metastable carbonaceous char formation. The third peak at temperatures above 650 °C proves the presence of residual char even with the presence of ZnO particles [28].

The non-irradiated samples do not present relevant alterations in the DTG plots. The most notorious changes were observed in irradiated samples, where the intensity reduction of the first signal for the composites, with respect to the neat epoxy, was observed. Similar behavior was presented at the highest temperatures (>650 °C).

The irradiation treatment alters the thermal stability of the epoxy, even in the presence of ZnO particles. The irradiation also seems to promote some molecular degradation of the resin and alters the interaction between the inorganic particles and the epoxy.

Figure 5 shows the DMA results of neat epoxy and epoxy-ZnO composites as a function of temperature. The DMA results are expressed as loss modulus, describing the sample's viscous part transferred into heat.

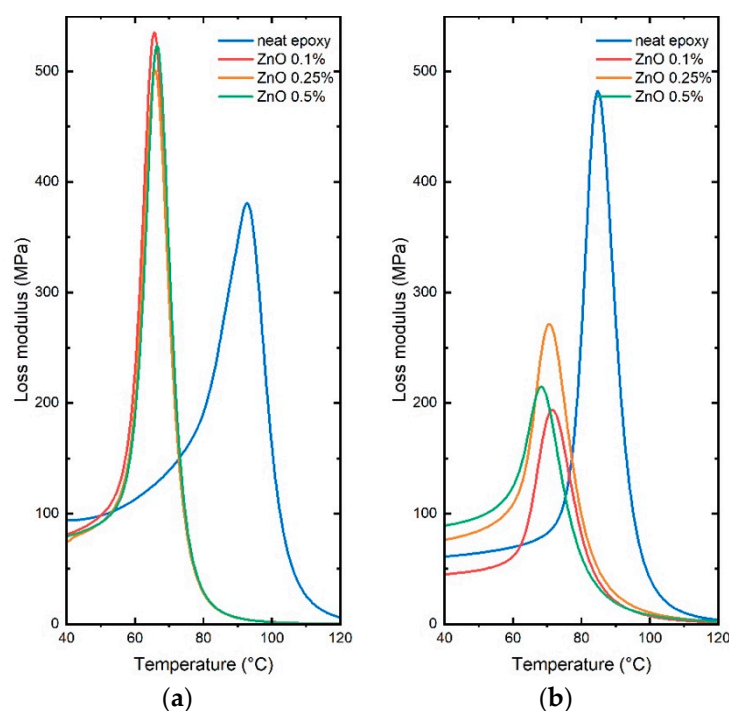


Figure 5. Loss modulus for ZnO-epoxy composite at 0.5 wt% (a) before and (b) after UV and gamma irradiation.

Concerning non-irradiated samples (Figure 5a), the modulus of loss of neat epoxy (94 MPa) is notoriously higher than that of epoxy-ZnO composites (~80 MPa). Additionally, it is evident that the peak position of the neat epoxy shifts towards temperatures well above the composites. The neat epoxy peak is 92 °C, while the peaks of the composites are between 65 and 66 °C, approximately. This represents a difference of almost 30 °C.

The reduction in the loss modulus in the composites can be attributed to the presence of ZnO particles, which restrict the molecular movement of the polymeric matrix. The displacement of the peaks towards lower temperatures would indicate a significant reduction in the energy wasted in the viscoelastic transformation, which may be promoted by a low matrix–reinforcement molecular interaction or by the agglomeration (poor dispersion) of ZnO particles, which decreases its thermal performance.

After the irradiation treatment (Figure 5b), the epoxy resin shows a considerable increase in peak intensity, contrary to what was observed in the epoxy-ZnO composites, which were notably reduced. The degradation of the resin could promote an increase in the intensity of the peak. In the case of composites, the reduction in the intensity of the peaks would represent a short transition region, which implies that the polymeric chains have a

greater capacity for movement, probably due to certain degradation phenomena induced during the irradiation treatment.

On the other hand, the loss modulus increases remarkably with increasing ZnO particle content, which is the opposite of the expected effect since a reduction in the loss modulus would represent an increase in the stiffness of the material. In this sense, the degradation promoted by the irradiation treatment would affect the matrix–reinforcement interaction, which would explain the displacement of the peaks towards a lower temperature with the increase in the ZnO content.

3.3. Mechanical Performance of Epoxy-ZnO Composite

Figure 6 represents the stress–strain curves of the samples having a concentration equal to 0.1 wt%, 0.25 wt% and 0.5 wt% in ZnO nanoparticles before gamma and UV irradiation. It thus makes it possible to study the evolution of the mechanical properties according to the increase in the quantity of nanoparticles. Tables 4 and 5 show the flexural properties of epoxy-ZnO composites before and after irradiation, respectively.

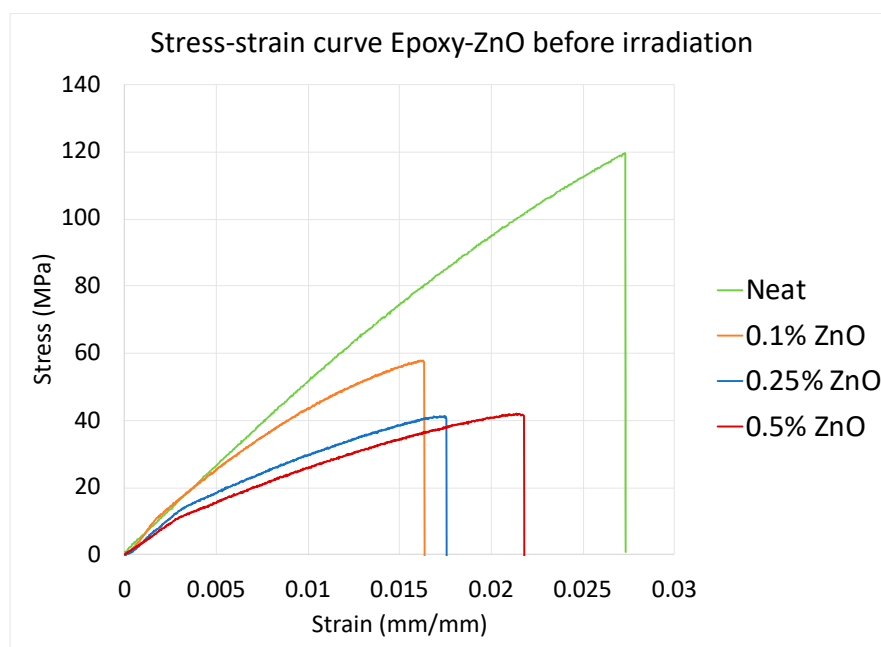


Figure 6. Stress–strain curves for epoxy-ZnO composites before irradiation.

Table 4. Flexural properties of epoxy-ZnO composites before irradiation.

Composite	Ultimate Strength (MPa)	Ultimate Strain	Flexural Modulus (GPa)
Neat epoxy	112.13 ± 6.2	0.029 ± 0.001	4.3 ± 0.33
0.1%	65.81 ± 7.9	0.016 ± 0.001	4.9 ± 0.49
0.25%	51.10 ± 1.7	0.017 ± 0.003	3.2 ± 0.63
0.5%	48.55 ± 12.9	0.021 ± 0.001	2.9 ± 0.47

Table 5. Flexural properties of epoxy-ZnO composites after irradiation.

Composite	Ultimate Strength (MPa)	Ultimate Strain	Flexural Modulus (GPa)
Neat epoxy	38.01 ± 4.6	0.051 ± 0.004	0.77 ± 0.16
0.1%	28.71 ± 1.5	0.074 ± 0.003	0.48 ± 0.02
0.25%	27.70 ± 6.69	0.092 ± 0.027	0.30 ± 0.13
0.5%	25.11 ± 8.45	0.062 ± 0.029	0.29 ± 0.01

According to these results, it is possible to notice that the maximum strength decreases even if the quantity of nanoparticles increases. Stiffness remains constant. This can be explained by the fact that ZnO nanofillers tend to agglomerate [20].

These samples are then exposed to gamma and UV rays, and then subjected to the same bending tests as before. The results are presented in Figure 7, thus making it possible to examine the influence of irradiation on the mechanical properties.

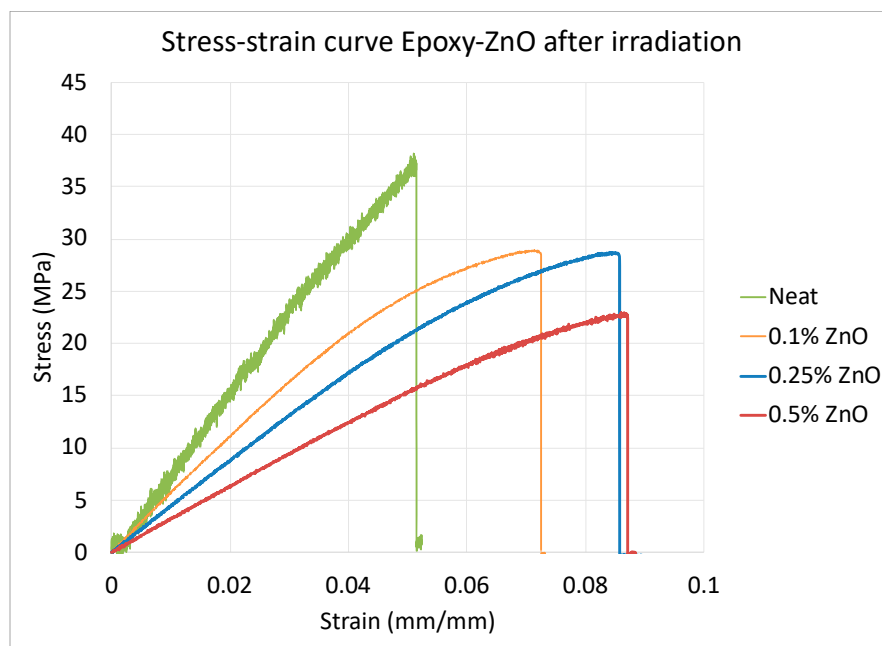


Figure 7. Stress–strain curves for epoxy-ZnO composites after irradiation.

4. Discussion

UV and gamma rays have a strong impact on the mechanical properties of the samples. Comparing Figures 6 and 7, the strength of the neat epoxy diminishes 60% and for the ZnO reinforced resins, diminution is at least 45%. When polymers are exposed to sunlight, most of them become weaker and softer due to the degradation of the polymer chains. UV and gamma rays can cause ionization and produce free radicals. These result from the breaking of carbon bonds, which are the primary bonds of thermoset resins. Typically, after irradiation, the content of C–C bonds reduces and the content of C–O and C=O bonds rises, indicating the increase in the oxidation of the material, since oxidative degradation of epoxy happens on the surface [25]. Other thermoset polymers, such as PMMA, when exposed to high energy particles produce bond breaking and create reactive radicals, promoting chain transfer reactions. Consequently, thermoset polymers have a new morphology, which can lead to compaction and therefore an alteration on the pristine mechanical properties [13,14].

It can be inferred that gamma and UV rays have a completely different effect depending on the absence or presence of ZnO nanoparticles. Reduction in mechanical properties is lower in epoxy-ZnO composites than the neat resin. In this study, the resin polymer chains are degraded by UV and gamma radiation in such a manner that for neat epoxy, stiffness is reduced 80% and, for epoxy-ZnO composites, stiffness is reduced in one magnitude order. Decrease in flexural modulus is related to the rupture of C–C and C–H bonds, diminishing the crosslinking points [25].

ZnO nanofillers, as well as other ones studied recently [21,29], enrich the irradiation performance of epoxy resins and moderate the oxidative mechanism through free radical scavenging [21,22]. Free radical scavenging is crucial because normally, in the presence of oxygen, peroxy radicals can form. These peroxy radicals have the ability to extract hydrogen atoms from the thermoset chain, highly contributing to polymer degradation. The free radical scavenging also depends on the structural defects of the nanofillers [21,22,30]. In the

case of carbon-based nanofillers (nanotubes, graphene oxide) and metal–organic nanoparticles (UIO-66-OH), it has been confirmed that porous morphology boosts the free radical scavenging ability. The ZnO nanoparticles used in this study have a commonly known wurtzite hexagonal phase. Then, if either a nanoporous ZnO phase or nanoparticle network with a super-specific surface area could be obtained, a better free radical scavenging would be expected, and therefore, an upgrade of the polymer degradation mechanism.

It has been proven that ZnO particles serve as crosslink inhibitors, avoiding the free movement and deformation of the polymer chains, providing thermoset resins with more ductile performance and tougher behavior [18,19]. ZnO nanoparticles act as energy-absorbing centers upon exposure to UV and gamma rays. Therefore, the kinetics of the ZnO nanoparticles are greater and lead to the redistribution of the nanoparticles within the polymer chain. The crosslinks between the polymer chains inside epoxy resin were broken by the incident UVA energy and become more flexible and tough, thus, polymer chains become more mobile and elastic and large deformations can be expected (as shown in Figure 7) [21,23,25]. The high-energy gamma rays dissociate the molecular chains of the thermoset resin, and then reactive free radicals are generated. These radicals keep attacking the polymer chains, causing more degradation. As a composite is damaged, cracks will redirect their path if they confront rigid particles. Then, the introduction of the ZnO nanofiller reduces the damage rate, causing a lower impact on ultimate strength and an increment in elongation [27]. Moreover, it has been proven that a decrease in flexural strength is also linked to superficial oxidation for the aromatic groups of epoxies when they are exposed to gamma irradiation [21,25,29].

5. Conclusions

The degradation of epoxy resin and ZnO-epoxy composite under UV and gamma irradiation was discussed. TGA, DMA and bending tests were carried out to estimate the impact of irradiation on this type of nanocomposite.

After irradiation, the thermal decomposition Td1 of the epoxy-ZnO composite is still higher than that of the neat epoxy. The T_{dmax} was increased on epoxy-ZnO composites because the ZnO nanoparticles inhibited the movement of the chain segments.

Regarding the DMA tests after irradiation, all the samples lost rigidity after adding nanoparticles. However, the sample with 0.1 wt% of ZnO nanoparticles has the highest storage modulus, so it is the most rigid. The irradiation promotes molecular degradation of the epoxy resin and alters the interaction between the inorganic particles and the epoxy chains.

Bending tests show that gamma and UV rays strongly impact the mechanical properties of epoxy-ZnO composites. Strength is reduced by at least 45%, and stiffness is reduced to 10 to 20% of its original value. Thus, the sample containing 0.1 wt% of ZnO nanoparticles is the most suitable for (i) mechanical purposes and (ii) resistance to UV and gamma irradiation.

For spacecraft design purposes, ZnO-epoxy can be used as polymer matrix candidate for carbon-reinforced plastics (CFRP). The irradiation dose 10 kGy is expected for a mission life of 5 years. Mechanical properties were reduced to less than 50% of their original values, which is in agreement with an End-of-Life (EoL) product expectancy.

Further work considers carrying out the same analyses on a similar resin but with other nanoparticles (graphene, carbon nanotubes and metakaolin).

6. Patents

There are no patents resulting from the work reported in this manuscript.

Author Contributions: Conceptualization, M.T.; methodology, M.T.; formal analysis, L.B. and A.V.R.-R.; investigation, L.B. and A.V.R.-R.; resources, E.A.F.-U.; data curation, L.B. and A.V.R.-R.; writing—original draft preparation, M.T.; writing—review and editing, A.V.R.-R. and E.A.F.-U.; supervision, E.A.F.-U.; project administration, M.T.; funding acquisition, M.T. and E.A.F.-U. All authors have read and agreed to the published version of the manuscript.

Funding: This research was funded by CONACYT, grant number 257458 and 275783, and the APC was funded by CONACYT, grant number 257458.

Data Availability Statement: This study did not report any data.

Acknowledgments: Authors thank the participation of Tomas J. Madera-Santana from CIAD (Centro de Investigación en Alimentación y Desarrollo) and Rodrigo Meléndrez-Amavizca from UNISON (University of Sonora) for the irradiation process. Authors also thank Nayeli Camacho-Tapia for advising on the ZnO particle preparation and Perla Alcántara for thermal characterization support.

Conflicts of Interest: The authors declare no conflict of interest. The funders had no role in the design of the study; in the collection, analyses, or interpretation of data; in the writing of the manuscript, or in the decision to publish the results.

References

1. Franco-Urquiza, E.A.; Dollinger, A.; Torres-Arellano, M.; Piedra, S.; Llanas, P.I.A.; Rentería-Rodríguez, V.; Pérez, C.Z. Innovation in Aircraft Cabin Interior Panels Part I: Technical Assessment on Replacing the Honeycomb with Structural Foams and Evaluation of Optimal Curing of Prepreg Fiberglass. *Polymers* **2021**, *13*, 3207. [[CrossRef](#)]
2. Franco-Urquiza, E.A.; Llanas, P.I.A.; Rentería-Rodríguez, V.; Saleme, R.S.; Aguilar, R.R.; Pérez, C.Z.; Torres-Arellano, M.; Piedra, S. Innovation in Aircraft Cabin Interior Panels. Part II: Technical Assessment on Replacing Glass Fiber with Thermoplastic Polymers and Panels Fabricated Using Vacuum Forming Process. *Polymers* **2021**, *13*, 3258. [[CrossRef](#)] [[PubMed](#)]
3. Torres-Arellano, M.; Bolom-Martínez, M.d.J.; Franco-Urquiza, E.A.; Pérez-Mora, R.; Jiménez-Arévalo, O.A.; Olivier, P. Bearing Strength and Failure Mechanisms of Riveted Woven Carbon Composite Joints. *Aerospace* **2021**, *8*, 105. [[CrossRef](#)]
4. Wong, T.; Tam, W.; Etches, J.A.; Wang, W.; Leng, J.; Lau, K. Feasibility of using ZnO/epoxy filled hollowed glass fibres (HGFs) for UV resistant polymer composites. *Mater. Lett.* **2014**, *128*, 220–223. [[CrossRef](#)]
5. Mehrparvar, A. *Cubesat Design Specifications Rev. 13*; California Polytechnic State University: San Luis Obispo, CA, USA; Stanford University: Stanford, CA, USA, 2014.
6. Corpino, S.; Caldera, M.; Nichele, F.; Masoero, M.; Viola, N. Thermal design and analysis of a nanosatellite in low earth orbit. *Acta Astronaut.* **2015**, *115*, 247–261. [[CrossRef](#)]
7. Niaki, K.S.; Anvari, A.; Farhani, F. Aluminum and composite materials for satellite structures—A comparison of thermal performance. *Mater. Sci. Res. India* **2007**, *4*, 25–34. [[CrossRef](#)]
8. Diao, F.; Zhang, Y.; Liu, Y.; Fang, J.; Luan, W. g-Ray irradiation stability and damage mechanism of glycidyl amine epoxy resin. *Nucl. Instrum. Methods Phys. Res. Sect. B* **2016**, *383*, 227–233. [[CrossRef](#)]
9. Armstrong, T.W.; Colborn, B.L. *Evaluation of Trapped Radiation, Model Uncertainties for Spacecraft Design*; Science Applications International Corporation: Prospect, TN, USA, 2000; pp. 1–47.
10. Bath, B.R.; Upadhyaya, N.; Kulkarni, R. Total radiation dose at geostationary orbit. *IEEE Trans. Nucl. Sci.* **2005**, *52*, 530–534. [[CrossRef](#)]
11. Condruz, M.R.; Voicu, L.R.; Puscasu, C.; Vintila, I.S.; Sima, M.; Deaconu, M.; Dragasanu, L. Composite material designs for lightweight space packaging structures. *INCAS Bull.* **2018**, *10*, 13–25.
12. Piedra, S.; Torres, M.; Ledesma, S. Thermal Numerical Analysis of the Primary Composite Structure of a CubeSat. *Aerospace* **2019**, *6*, 97. [[CrossRef](#)]
13. Quero, G.; Vaiano, P.; Fienga, F.; Giaquinto, M.; Di Meo, V.; Gorine, G.; Casolaro, P.; Campajola, L.; Breglio, G.; Crescitelli, A.; et al. A novel Lab-on-Fiber Radiation Dosimeter for Ultra-high Dose Monitoring. *Sci. Rep.* **2018**, *8*, 17841. [[CrossRef](#)] [[PubMed](#)]
14. Ravotti, F. Dosimetry Techniques and Radiation Test Facilities for Total Ionizing Dose Testing. *IEEE Trans. Nucl. Sci.* **2018**, *65*, 1140–1463. [[CrossRef](#)]
15. Torres, M.; Franco-Urquiza, E.A.; González-García, P.; Bárcena-Balderas, J.; Piedra, S.; Madera-Santana, T.; Meléndrez-Amavizca, R.; Quintana-Owen, P. Characterization of Epoxy-Nanoparticle Composites Exposed to Gamma & UV Radiation for Aerospace Applications. *Nano Hybrids Compos.* **2019**, *27*, 53–65. [[CrossRef](#)]
16. Qin, L.; Shing, C.; Sawyer, S.; Dutta, P.S. Enhanced ultraviolet sensitivity of zinc oxide nanoparticle photoconductors by surface passivation. *Opt. Mater.* **2011**, *33*, 359–362. [[CrossRef](#)]
17. Torres, M.; Rentería, A.V.; Alcántara, P.I.; Franco-Urquiza, E. Mechanical properties and fracture behaviour of agave fibers bio-based epoxy laminates reinforced with zinc oxide. *J. Ind. Text.* **2020**, *51*, 5847S–5868S. [[CrossRef](#)]
18. Wong, T.; Lau, K.; Tam, W.; Leng, J.; Etches, J.A. UV resistibility of a nano-ZnO/glass fibre reinforced epoxy composite. *Mater. Des.* **2014**, *56*, 254–257. [[CrossRef](#)]
19. Wong, T.; Lau, K.; Tam, W.; Leng, J.; Wang, W.; Li, W.; Wei, H. Degradation of nano-ZnO particles filled styrene-based and epoxy-based SMPs under UVA exposure. *Compos. Struct.* **2015**, *132*, 1056–1064. [[CrossRef](#)]
20. Al Naim, A.; Alnaim, N.; Ibrahim, S.S.; Metwally, S.M. Effect of gamma irradiation on the mechanical properties of PVC/ZnO polymer nanocomposite. *J. Radiat. Res. Appl. Sci.* **2017**, *10*, 165–171. [[CrossRef](#)]

21. Wang, S.; Song, L.; Liu, S.; Pei, X.; Zhao, Y.; Min, C.; Shao, R.; Ma, T.; Yin, Y.; Xu, Z.; et al. Metal-organic framework nanoparticles as a free radical scavenger improving the stability of epoxy under high dose gamma radiation. *Polym. Degrad. Stab.* **2023**, *207*, 110231. [[CrossRef](#)]
22. Wang, H.; Li, N.; Xu, Z.; Tian, X.; Mai, W.; Li, J.; Chen, C.; Chen, L.; Fu, H.; Zhang, X. Enhanced sheet-sheet welding and interfacial wettability of 3D graphene networks as radiation protection in gamma-irradiated epoxy composites. *Compos. Sci. Technol.* **2018**, *157*, 57–66. [[CrossRef](#)]
23. Chen, Y.; Ding, H.; Sun, S. Preparation and Characterization of ZnO Nanoparticles Supported on Amorphous SiO₂. *Nanomaterials* **2017**, *7*, 217. [[CrossRef](#)] [[PubMed](#)]
24. Camacho, N.; May-Crespo, J.F.; Rojas-Trigos, J.B.; Martínez, K.; Marín, E.; Mondragón-Rodríguez, G.C. Thermal properties and degradation kinetics of epoxy- γ -alumina and epoxy-zinc oxide lightweight composites. *Rev. Mex. Fís.* **2020**, *66*, 479–489. [[CrossRef](#)]
25. Chen, K.; Zhao, X.; Zhang, F.; Wu, X.; Huang, W.; Liu, W.; Wang, X. Influence of gamma irradiation on the molecular dynamics and mechanical properties of epoxy resin. *Polym. Degrad. Stab.* **2019**, *168*, 108940. [[CrossRef](#)]
26. Wachowski, L.; Hofman, M. Application of TG-DTG analysis in the study of the ammoxidised carbon materials. *J. Therm. Anal. Calorim.* **2006**, *83*, 379–383. [[CrossRef](#)]
27. Franco-Urquiza, E.A.; May-Crespo, J.F.; Escalante-Velázquez, C.A.; Pérez-Mora, R.; González-García, P. Thermal Degradation Kinetics of ZnO/polyester Nanocomposites. *Polymers* **2020**, *12*, 1753. [[CrossRef](#)] [[PubMed](#)]
28. Parimalam, M.; Islam, M.R.; Yunus, R.M. Effects of nano- and micro-sized inorganic fillers on the performance of epoxy hybrid nano coatings. *Polym. Polym. Compos.* **2019**, *27*, 82–91.
29. Liu, Y.; Zhang, S.; Pei, X.; Shi, H.; Li, D.; Xu, Z.; Li, S.; Xue, Y.; Song, L. Free radical scavenging behavior of multidimensional nanomaterials in γ -irradiated epoxy resin and mechanical and thermal performance of γ -irradiated composites. *Compos. Part C* **2021**, *4*, 100095. [[CrossRef](#)]
30. Yan, M.; Liu, L.; Chen, L.; Li, N.; Jiang, Y.; Xu, Z.; Jing, M.; Hu, Y.; Liu, L.; Zhang, X. Radiation resistance of carbon fiber-reinforced epoxy composites optimized synergistically by carbon nanotubes in interface area/matrix. *Compos. Part B* **2019**, *172*, 447–457. [[CrossRef](#)]

Disclaimer/Publisher's Note: The statements, opinions and data contained in all publications are solely those of the individual author(s) and contributor(s) and not of MDPI and/or the editor(s). MDPI and/or the editor(s) disclaim responsibility for any injury to people or property resulting from any ideas, methods, instructions or products referred to in the content.